

Global solution of viscous accretion disk around rotating compact objects: a pseudo-general-relativistic study

Banibrata Mukhopadhyay¹ & Shubhrangshu Ghosh²

¹ *Inter-University Centre for Astronomy and Astrophysics, Post Bag 4, Ganeshkhind, Pune-411007, India*

² *Department of Physics and Center for Theoretical Studies, Indian Institute of Technology, Kharagpur-721302, India*

20 August 2010

Accepted for publication in *Monthly Notices of the Royal Astronomical Society*

ABSTRACT

We study the solution of viscous accretion disks around rotating compact/central object having hard surface i.e. neutron star, strange star and any other highly gravitating objects. We choose pseudo-Newtonian approach to describe the relativistic accretion disk. For this purpose, a new pseudo-Newtonian potential is established which is applicable to describe the relativistic properties of star and its disk. As we know, the Hartle-Thorne metric can describe geometry of star as well as the space-time out-side of it, we use this metric to establish our potential. Our potential reproduces the marginally stable orbit exactly as that of general relativity. It also reproduces the marginally bound orbit and specific mechanical energy at the marginally stable orbit with at most 4% and 10% error respectively. Using this potential we study the global parameter space of the accretion disk. Thus, we find out the physical parameter regime, for which the stable accretion disk can be formed around gravitating object with hard surface. We also study, how the fluid properties get changed with different rotations of the central star. We show that with the change of rotation to the central object, the valid disk parameter region dramatically changes. We also show the effect of viscosity to the fluid properties of the disk. Subsequently, we give a theoretical prediction

of kHz QPO, at least for one out of a pair, for a fast rotating compact object as 4U 1636-53.

Key words: accretion, accretion disk — stars: rotation — hydrodynamics — gravitation — shock waves — X-rays: binaries

1 INTRODUCTION

For over last three decades, fluid dynamical study of accretion disks around compact object is indeed a topic extensively discussed, mostly for black holes (Abramowicz et al. 1988, 1996; Abramowicz & Kato 1989; Chakrabarti 1990, 1996a,b,c; Narayan & Yi 1994; Narayan et al. 1997, 1998; Kato et al. 1998; Sponholz & Molteni 1994; Peitz & Appl 1997; Gammie & Popham 1998; Popham & Gammie 1998; Miwa et al. 1998; Lu & Yuan 1998; Manmoto 2000) and a few for neutron stars (Chakrabarti & Sahu 1997; Mukhopadhyay 2000, 2002a; Popham & Sunyaev 2001). Though in some of the cases authors use full general relativistic approach, in most of the cases the approaches are pseudo-Newtonian. In the pseudo-Newtonian method, they use simple non-relativistic equations to describe the disk with the appropriate choice of modified gravitational force which takes care about the geometry of back-ground space-time. There are a number of basic differences between the accretion disk around black hole and any other gravitating objects namely neutron star, white dwarf, strange star and other gravitating stars particularly at the inner edge of the disk. (1) While the black hole has event horizon, other gravitating objects mentioned above have hard surface. Thus, whereas in the case of other gravitating object close to the surface the matter speed must be subsonic, for black holes the matter speed is supersonic. (2) In case of other gravitating object that has hard surface, the matter comes into contact with its outer surface. Thus, there is an obvious effect of dragging to the exterior space-time due to its rotation. In terms of general relativity, corresponding space-time metric should be the solution for interior as well as exterior to it. Therefore, it is necessary to consider the 'dragging effect' of rotating gravitating star (particularly for neutron star, where the relativistic effect is very important) to the space-time. In case of black hole, which does not have hard surface, this effect comes to the space-time automatically through the 'Lense-Thirring drag' from the Kerr geometry which does not describe any physics interior to the horizon. (3) Further, the overall temperature as well as the luminosity of the disk is expected to be high in the cases of other gravitating star particularly for neutron star with respect to that of black hole (Mukhopadhyay 2000,

2002a) for a particular accretion rate. If the same parameters are chosen for the infalling matter towards black hole and other gravitating objects separately, at same accretion rate, the maximum temperature in the disk around black hole will be lower at least a few factors times. Thus, in the disk around neutron star, expected generation/absorption of nuclear energy is higher than that of black hole (Mukhopadhyay 2002a). As there is a clear distinction between accretion disks around black hole and other gravitating objects, hereinafter, we will call the class of gravitating objects having hard surface as GOHS to distinguish from black hole. GOHS can be meant as neutron star, strange star, white dwarf and any other highly gravitating objects where disk may form. As the radius of white dwarf is very large, the general relativity is not much important in the accretion disk around it. But our discussions will be generally true for disk around any kind of GOHS.

Mukhopadhyay (2002a) has studied the accretion disk around weakly magnetized slowly rotating neutron stars, and found that the temperature of the inner disk is significantly higher than the case of black holes. Prasanna & Mukhopadhyay (2003) have described the accretion disk with the inclusion of 'Coriolis' effect. They have shown that the rotational effect of compact object to the accretion disk can be approximately reproduced with the use of Coriolis effect. They have done perturbative analysis and shown that the *self-similar solutions* are well behaved for most of the parameter space. As no cosmic object is static, in this paper, our interest is to include the rotation of the neutron star, globally speaking rotation of GOHS, in a more proper manner and see its effect onto the disk. The recent observation tells about the evidence of millisecond pulsar (Strohmayer & Markwardt 2002) of frequency 582Hz for 4U 1636-53 which is the accreting LMXB. Therefore, it is important to consider the rotational effect of the GOHS to the disk. We approach our study in pseudo-Newtonian manner. So far, there is no pseudo-potential in the literature which can describe the accretion disk around GOHS. Thus, first of all we should establish such a potential useful for our work.

Shakura & Sunyaev (1973) first initiated the accretion disk modeling using simple Newtonian potential meant for non-rotating black holes. As the relativistic effects are extremely important near the compact objects, this potential can not describe the essential inner properties of the disk. Paczyński & Wiita (1980) modified this Newtonian potential in conformity with the Schwarzschild geometry, which can naturally reveal approximately the properties of disk around non-rotating black holes and GOHSs, even that of the inner most part of the disk. The potential can reproduce the radius of marginally stable orbit (x_s) and marginally

bound orbit (x_b), mechanical energy per unit mass at the last stable circular orbit (E_s) and viscous efficiency of the disk. The last two parameters agree within a 10% error but the first two cases exactly match with that of the Schwarzschild metric. Nowak & Wagoner (1991) proposed another potential for accretion disk around non-rotating black holes. This potential can also mimic approximately most of the properties of the disk governed by Schwarzschild geometry. However, angular and epicyclic frequency of the disk can be best analyzed with this potential. Artemova et al. (1996) proposed a couple of pseudo-potentials to describe accretion disk for rotating and non-rotating black holes. These potentials are well analyzed by a number of astrophysicists later (e.g. Lovas 1998; Semerák & Karas 1999). Very recently, Mukhopadhyay (2002b) and Mukhopadhyay & Misra (2003) prescribed some new potentials with which properties of accretion disk can be very well described in Kerr geometry. The more interesting fact lies in the methodology adopted by Mukhopadhyay (2002b) to describe a potential in the accretion disk, which can be used to derive the pseudo-potential for any metric according to the physics concerned. The potentials proposed by Mukhopadhyay & Misra (2003) can be used for the time-dependent simulation of accretion disk. But all the potentials are described either for the fluid dynamical study of disk around black hole or the study of temporal effect around compact objects. As the fluid properties of inner accretion disk are very much influenced by the nature of central gravitating object as mentioned above, it is essential to establish a pseudo-potential which can describe an accretion disk around GOHS. Although in case of black hole, the space-time can be described by Kerr geometry, but in the case of GOHS with slow rotation, the corresponding metric which can continuously describe the space-time inside and outside the star is Hartle-Thorne (hereinafter HT, Hartle & Thorne 1968). Thus, we should establish our potential according to HT metric.

Thus, we shall consider the general solutions for fluid disks around rotating GOHS. In order to consider a solution procedure, we will follow Chakrabarti (1996b) where the global solution for transonic accretion flows is studied around rotating black holes but in the case of weak viscosity. Here, we will consider the set of disk equations in terms of general viscous prescription and the accretion around GOHS. As we want to concentrate upon the features of the inner region, we shall restrict the study to 'sub-Keplerian' flow. We study, how does the rotation of GOHS affect on the global parameter space of accretion disk. We know that for the case of non-rotating compact object, the stable accretion disk forms only for a certain set of physical parameter. We would like to check how this parameter region gets affected, how does the steady disk structure change, with different values of the rotation to GOHS.

Once we have the clear picture about the parameter space, we will concentrate upon the fluid properties of the disk for different viscosity and how does the viscous fluid properties change with different rotations of GOHS.

Therefore, we are going to present a complete set of work on accretion disk around GOHS. In order to do so, in the next section, we will derive the required pseudo-Newtonian potential and establish its efficiency. In §3, we will present the basic equations of viscous accretion disk around GOHS. In §4 and §5, we will analyse the parameter space of the accretion disk around GOHS and corresponding properties of accreting fluid respectively. Finally we shall present our discussion and overall summary in §6.

2 PSEUDO-NEWTONIAN POTENTIAL AND ITS EFFICIENCY

Here, following Mukhopadhyay (2002b), we will derive the pseudo-Newtonian potential for accretion disk modeling around GOHS according to HT metric. The Lagrangian density for a particle in the HT geometry (neglecting the higher quadruple terms) at the equatorial plane ($\theta = \pi/2$) can be written as

$$2\mathcal{L} = - \left(1 - \frac{2M}{r} - \frac{2J^2}{r^4}\right) \dot{t}^2 + \left(1 - \frac{2M}{r} + \frac{2J^2}{r^4}\right)^{-1} \dot{r}^2 + r^2 \dot{\phi}^2 - \frac{4J}{r} \dot{\phi} \dot{t}, \quad (1)$$

where over-dots denote the derivative with respect to the proper-time τ and J denotes the angular momentum of GOHS. As the metric is valid only for slowly rotating stars, the rotation parameter J is restricted as $J \leq 0.5$. The geodesic equations of motion are

$$E = \text{constant} = \left(1 - \frac{2M}{r} - \frac{2J^2}{r^4}\right) \dot{t} + \frac{2J}{r} \dot{\phi}, \quad (2)$$

$$\lambda = \text{constant} = r^2 \dot{\phi} - \frac{2J}{r} \dot{t}. \quad (3)$$

For the particle with non-zero rest mass, $g_{\mu\nu} p^\mu p^\nu = -m^2$ (where p^μ is the momentum of the particles and $g_{\mu\nu}$ is the metric). Replacing the solution for \dot{t} and $\dot{\phi}$ from (2) and (3) into (1) gives a differential equation for r

$$\begin{aligned} \left(\frac{dr}{d\tau}\right)^2 &= \left(\frac{4h(r)J^2}{g(r)r^6} + \frac{16J^4}{g(r)r^{10}} - \frac{g(r)}{r^2}\right) \lambda^2 + \left(\frac{h(r)}{g(r)} + \frac{4J^2}{g(r)r^4}\right) E^2 \\ &+ \left(-\frac{4h(r)J}{g(r)r^3} - \frac{16J^3}{g(r)r^7}\right) E\lambda - g(r)m^2 = \Psi, \end{aligned} \quad (4)$$

where, $g(r) = \left(1 - \frac{2m}{r} + \frac{2J^2}{r^4}\right)$, $h(r) = \left(1 - \frac{2m}{r} - \frac{2J^2}{r^4}\right)$. Here, Ψ can be identified as an effective potential for the radial geodesic motion. The conditions for circular orbits are

$$\Psi = 0, \quad \frac{d\Psi}{dr} = 0. \quad (5)$$

Solving for E and λ from (5) we get

$$E = X(r), \quad (6)$$

$$\lambda = X(r) \sqrt{\frac{m^4 r^6 (-4J^2 + Mr^3)^2}{[-2J^3 m^2 + Jm^2 r^3 (-4m + 3r) + \sqrt{m^4 (5J^2 + Mr^3) (2J^2 + r^3 (-2M + r))^2}]^2}}, \quad (7)$$

where,

$$\begin{aligned} X(r) = & \frac{1}{m^2 r^3 (-4J^2 + Mr^3)} \left[2J^3 m^2 + Jm^2 (4M - 3r) r^3 \right. \\ & \left. - \sqrt{m^4 (5J^2 + Mr^3) (2J^2 + r^3 (-2M + r))^2} \right] \\ & \{ (-12J^4 m^2 r^2 + 2J^2 m^2 (9M - 7r) r^5 + m^2 M (3M - r) r^8 \\ & + 6Jr^2 \sqrt{m^4 (5J^2 + Mr^3) (2J^2 + r^3 (-2M + r))^2} / \\ & (36J^4 - r^6 (-3M + r)^2 + 12J^2 r^3 (-3M + 2r)) \}^{1/2}. \quad (8) \end{aligned}$$

Now as standard practice, we can define the Keplerian angular momentum distribution, $\lambda_K = \frac{\lambda}{E}$. Therefore, corresponding centrifugal force in HT geometry can be written as

$$\frac{\lambda_K^2}{r^3} = \frac{m^4 r^3 (-4J^2 + Mr^3)^2}{[-2J^3 m^2 + Jm^2 r^3 (-4m + 3r) + \sqrt{m^4 (5J^2 + Mr^3) (2J^2 + r^3 (-2M + r))^2}]^2} = F_r. \quad (9)$$

Thus from above, F_r can be identified as the gravitational force of rotating GOHS at the Keplerian orbit in an equatorial plane. If we choose $x = r/M$ (as $G = c = 1$) and $m = 1$, above expression reduces to

$$F = \frac{x^3 (-4J^2 + x^3)^2}{[-2J^3 + Jx^3 (-4 + 3x) + \sqrt{(5J^2 + x^3) (2J^2 + x^3 (-2 + x))^2}]^2}. \quad (10)$$

Also the above expression reduces to Paczyński-Wiita (1980) form for $J = 0$. Thus we propose that (10) is the most general form of the gravitational force corresponding to the pseudo-potential in accretion disk around GOHS at equatorial plane.

2.1 Comparison of the Results for Hartle-Thorne geometry and Pseudo-Potential

Now we will establish the validity of this potential. We would like to check, whether this potential can reproduce the values of marginally bound (x_b), marginally stable (x_s) orbits and mechanical energy per unit mass at x_s (E_s), as same as HT geometry or not.

In terms of the pseudo-potential, one can write the radial velocity (v), angular velocity (Ω) and angular momentum per unit mass (λ) for a Keplerian orbit in an accretion disk as (Lynden-Bell 1969, Pringle & Rees 1973, Shakura & Sunyaev 1973, Novikov & Thorne 1973, Paczyński & Wiita 1980),

$$v = \sqrt{x \frac{dV}{dx}}, \quad \Omega = \sqrt{\frac{1}{x} \frac{dV}{dx}}, \quad \lambda = \sqrt{x^3 \frac{dV}{dx}}. \quad (11)$$

At the marginally bound orbit, mechanical energy E reduces to zero and we get

$$\frac{v^2}{2} + V = \frac{x}{2} \frac{dV}{dx} + V = 0, \quad (12)$$

where, $V = \int F dx$, which can be used to calculate x_b for the potential. For the last stable orbit (x_s), $d\lambda/dx = 0$, for our pseudo-potential which gives

$$x^5 \left[-8J^4 + 2J^2(5 - 2x)x^3 + (x - 2)x^6 \right] \left[-240J^6 + (x - 6)x^9 + 8J^4x^3(12 + 5x) \right. \\ \left. + 2J^2x^6(20x - 33) + (24J^3 + 12Jx^3)\sqrt{(5J^2 + x^3)(2J^2 + (x - 2)x^3)^2} \right] = 0. \quad (13)$$

The solution of (13) gives the location of the last stable circular orbit (x_s). For any J , the value of x_s computed from the above equation (13), matches exactly with the radius of last stable circular orbit in HT geometry. In Table-1, 2 and 3, we list x_b , x_s and E_s respectively for the potential V and HT geometry for various values of J .

Table-1

Values of x_b

J	0	0.1	0.2	0.3	0.4	0.5
V	4	3.7862	3.5619	3.3255	3.0762	2.8135
HT	4	3.7954	3.5810	3.3557	3.118	2.8689
J	0	-0.1	-0.2	-0.3	-0.4	-0.5
V	4	4.2042	4.4	4.5885	4.77	4.9462
HT	4	4.1957	4.3838	4.5684	4.7397	4.9089

Table-2

Values of x_s

J	0	0.1	0.2	0.3	0.4	0.5
V & HT	6.0	5.6648	5.3107	4.9339	4.5299	4.0934
J	0	-0.1	-0.2	-0.3	-0.4	-0.5
V & HT	6.0	6.3189	6.6240	6.9170	7.1994	7.4724

Table-3

Values of E_s

J	0	0.1	0.2	0.3	0.4	0.5
V	-0.0625	-0.0664	-0.0711	-0.0769	-0.0843	-0.0943
HT	-0.0572	-0.0607	-0.0649	-0.0701	-0.0767	-0.0857
J	0	-0.1	-0.2	-0.3	-0.4	-0.5
V	-0.0625	-0.0592	-0.0563	-0.0538	-0.0516	-0.0497
HT	-0.0572	-0.0542	-0.0517	-0.0494	-0.0474	-0.0457

From Table-1, it is clear that for all values of J , V can reproduce the value of x_b in very good agreement with general relativistic (HT) results. The maximum error in x_b is $\sim 4\%$.

Table-2 indicates that V reproduces x_s exactly as that of HT geometry. Table-3 shows a maximum possible error in E_s is $\sim 10\%$. Thus, the potential V will produce a slightly larger luminosity than the general relativistic one in the accretion disk for a particular value of J . It is to be noticed that for counter-rotating GOHS, that is for retrograde orbits, the errors are less than those of co-rotating ones. Eventually, we can tell that our potential can describe approximately all the phenomena of that of HT geometry and can claim it as a good pseudo-potential to describe the relativistic accretion disk around the rotating GOHS, particularly close to the equatorial plane. Thus, for a thin disk or vertically averaged disk, this is an ideal pseudo-potential.

3 BASIC EQUATIONS OF ACCRETION DISK AND THEIR CONSEQUENCES

Here, throughout our calculations, we express the radial coordinate in unit of GM/c^2 , where M is mass of the compact object, G is the gravitational constant and c is the speed of light. We also express the velocity in unit of speed of light and the angular momentum in unit of GM/c . The equations to be solved are given below.

(1) Equation of continuity:

$$-4\pi x \Sigma v = \dot{M}, \tag{14}$$

where Σ is the vertically integrated density and \dot{M} is the accretion rate. Following Matsumoto et al. (1984), we can calculate the Σ as

$$\Sigma = I_n \rho_e h(x), \tag{15}$$

where ρ_e is the density at equatorial plane, $h(x)$ is the half-thickness of the disk and $I_n = \frac{(2^n n!)^2}{(2n+1)!}$, where n is the polytropic index. From the vertical equilibrium assumption, the half-thickness can be written as

$$h(x) = c_s x^{1/2} F^{-1/2}, \tag{16}$$

where c_s is the speed of sound.

(2) Radial momentum balance equation:

$$v \frac{dv}{dx} + \frac{1}{\rho} \frac{dP}{dx} - \frac{\lambda^2}{x^3} + F(x) = 0, \tag{17}$$

where the flow is chosen adiabatic with the equation of state to be $P = k\rho^\gamma$ and $c_s^2 = \frac{\gamma P}{\rho}$.

(3) Azimuthal momentum balance equation: Here, we will follow Chakrabarti (1996a) to

express the viscous dissipation Q^+ in terms of shear stress $W_{x\phi}$. Because of this viscous dissipation, the angular momentum varies in accretion disk. Thus, $W_{x\phi} = -\alpha(I_{n+1}P + I_n v^2 \rho)h(x)$ and $Q^+ = \frac{W_{x\phi}^2}{\eta}$, η is coefficient of viscosity and α is Shakura-Sunyaev (1973) viscosity parameter. Thus the equation to be

$$v \frac{d\lambda}{dx} = \frac{1}{\rho h(x)x} \frac{d}{dx} \left[x^2 \alpha \left(\frac{I_{n+1}}{I_n} P + v^2 \rho \right) h(x) \right]. \quad (18)$$

(4) Entropy equation: According to the mixed shear stress (Chakrabarti 1996a), $Q^+ = -\alpha(I_{n+1}P + I_n v^2 \rho)h(x)x \frac{d\Omega}{dx}$. For simplicity, we also consider the heat lost is proportional to the heat gained by the flow. Thus the equation to be

$$\Sigma v T \frac{ds}{dx} = \frac{v h(x)}{\Gamma_3 - 1} \left(\frac{dP}{dx} - \Gamma_1 \frac{P}{\rho} \frac{d\rho}{dx} \right) = Q^+ - Q^- = f Q^+, \quad (19)$$

where s is entropy density and f is cooling factor which is close to 0 and 1 for the flow with efficient and inefficient cooling respectively. Following Cox & Giuli (1968), we can define

$$\Gamma_3 = 1 + \frac{\Gamma_1 - \beta}{4 - 3\beta}, \quad \Gamma_1 = \beta + \frac{(4 - 3\beta)^2(\gamma - 1)}{\beta + 12(\gamma - 1)(1 - \beta)}, \quad \beta = \frac{\rho k T / \mu m_p}{\bar{a} T^4 / 3 + \rho k T / \mu m_p}. \quad (20)$$

Here, β (ratio of gas pressure to total pressure) close to 0 for radiation dominated flow (highly relativistic flow) and close to 1 for gas dominated flow. Now combining (14),(17), (18) and (19), we get

$$\frac{dv}{dx} = \frac{f_1(x, v, c_s)}{f_2(v, c_s)}, \quad (21)$$

where,

$$f_1(x, v, c_s) = \left[c_s^2 \left(\frac{3}{2x} - \frac{1}{2F} \frac{dF}{dx} \right) - \gamma \left(F - \frac{\lambda^2}{x^3} \right) \right] \left[v(\Gamma_1 + 1) - \frac{4\alpha\Lambda}{v(3\gamma - 1)} \right] - \left[\frac{2\alpha c_s^2}{(3\gamma - 1)xv} + \frac{\alpha v}{x} - \frac{2\lambda}{x^2} \right] \Lambda + \left(\frac{3}{2x} - \frac{1}{2F} \frac{dF}{dx} \right) v c_s^2 (\Gamma_1 - 1), \quad (22)$$

$$f_2(v, c_s) = \left[1 - \frac{2c_s^2}{(3\gamma - 1)v^2} \right] \alpha \Lambda - c_s^2 (\Gamma_1 - 1) + \left(\gamma v - \frac{c_s^2}{v} \right) \left[v(\Gamma_1 + 1) - \frac{4\alpha\Lambda}{(3\gamma - 1)v} \right] \quad (23)$$

and $\Lambda = \gamma(\Gamma_3 - 1) f \alpha \left(\frac{I_{n+1}}{I_n} \frac{c_s^2}{\gamma} + v^2 \right)$.

As far away from the black hole, $v < c_s$ and close to it, $v > c_s$, there must be an intermediate location, where the denominator of (21) must be vanished. To have a smooth solution, at that location, numerator has to be zero. This location is called the sonic point or critical point (x_c). The existence of sonic location plays an important role in accretion phenomena. Although, in case of accretion flow of matter around black hole sonic point must exist, for that around GOHS (say, neutron star) it is not always necessary (Mukhopadhyay 2002a). When shock forms in an accretion disk around a neutron star (Chakrabarti & Sahu

1997, Mukhopadhyay 2002a), sonic points play an important role. From the global study of the sonic points in an accretion disk, one can understand about the stability of physical parameter region, which we will discuss in the next section.

Now, when the sonic point exists in an accretion disk around GOHS, $f_2(v_c, c_{sc}) = 0$ at $x = x_c$. Thus at that location Mach number can be written as

$$M_c^2 = \frac{\mathcal{B} + \sqrt{\mathcal{B}^2 - 4\mathcal{A}\mathcal{C}}}{2\mathcal{A}}, \quad (24)$$

where

$$\begin{aligned} \mathcal{A} &= \alpha^2 \gamma f(\Gamma_3 - 1) + \gamma(\Gamma_1 + 1) - \frac{4\alpha^2 f(\Gamma_3 - 1)\gamma^2}{3\gamma - 1}, \\ \mathcal{B} &= 2\Gamma_1 - \frac{4\alpha^2 \gamma f(\Gamma_3 - 1)}{3\gamma - 1} \left(1 - \frac{I_{n+1}}{I_n}\right), \\ \mathcal{C} &= \frac{2\alpha^2 f(\Gamma_3 - 1) I_{n+1}}{3\gamma - 1} \frac{I_n}{I_n}. \end{aligned} \quad (25)$$

Subsequently, at $x = x_c$, $f_1(x_c, v_c, c_{sc}) = 0$. Thus, using (24) we can eliminate v_c from $f_1(x_c, v_c, c_{sc}) = 0$ and get an algebraic equation for c_{sc} and x_c , which we can solve to find out sound speed at sonic location. To find out $\frac{dv}{dx}|_c$, we apply l'Hospital's rule to (21). In order to understand the fluid properties in accretion disk, we have to solve (21) with an appropriate boundary condition. Also, integrating (18), we get the angular momentum of the accreting matter as

$$\lambda = \frac{\alpha x c_s^2}{v} \left(\frac{2}{3\gamma - 1} + M^2 \right) + \lambda_{in}, \quad (26)$$

where M is the Mach number of the flow and λ_{in} is the angular momentum at the inner edge of accretion disk.

Now integrating (14) and (17), we can write the entropy and energy of the flow at sonic point as

$$\dot{\mathcal{M}}_c = x_c^{3/2} F_c^{-1/2} (\gamma + 1)^{q/2} \left(\frac{\frac{\lambda^2}{x_c^3} - F_c}{\frac{1}{F_c} \frac{dF}{dx}|_c - \frac{3}{x_c}} \right)^{\frac{\gamma}{\gamma-1}} \quad (27)$$

and

$$E_c = \frac{2\gamma}{(\gamma - 1)} \left(\frac{\frac{\lambda^2}{x_c^3} - F_c}{\frac{1}{F_c} \frac{dF}{dx}|_c - \frac{3}{x_c}} \right) + V_c + \frac{\lambda^2}{2x_c^2}, \quad (28)$$

where $V_c = (\int F dx)|_c$ and $q = \frac{(\gamma+1)}{2(\gamma-1)}$. It can be mentioned that, disk entropy and accretion rate are related by a simple relation as $\dot{\mathcal{M}} = (\gamma K)^n \dot{M}$. While \dot{M} is a conserved quantity for the particular accretion flow, $\dot{\mathcal{M}}$ is not, as it contains K^n which carries the entropy information that is not conserved in a dissipative system. As a boundary condition for the

particular flow, we have to supply the sonic energy E_c . Then from (28), we can find out the sonic location x_c . Therefore, knowing x_c one can easily find out the fluid velocity and sound speed at the sonic point from $f_1 = f_2 = 0$ with the help of (24) for a particular accretion flow. These have to be supplied as further boundary conditions of the flow.

Now let us come to the issue of the formation of shock. Mukhopadhyay (2002a) showed that in accretion disk around neutron star, double shock is very natural in certain physical situations. Here, whenever we mention the shock, we will mean Rankine-Hugoniot shock (Landau & Lifshitz 1987). If we generalise the conditions to form a shock in an accretion disk given by Chakrabarti (1989) for rotating GOHS, we get

$$\frac{1}{2}M_+^2 c_{s+}^2 + n c_{s+}^2 = \frac{1}{2}M_-^2 c_{s-}^2 + n c_{s-}^2, \quad (29)$$

$$\frac{c_{s+}^\nu}{\dot{M}_+} \left(\frac{2\gamma}{3\gamma-1} + \gamma M_+^2 \right) = \frac{c_{s-}^\nu}{\dot{M}_-} \left(\frac{2\gamma}{3\gamma-1} + \gamma M_-^2 \right), \quad (30)$$

$$\dot{M}_+ > \dot{M}_-, \quad (31)$$

where

$$\dot{M} = M c_s^{2(n+1)} \frac{x_s^{3/2}}{\sqrt{F_s}}. \quad (32)$$

Here, subscript ‘-’ and ‘+’ indicate the quantities just before and after the shock respectively, x_s indicates the shock location and $\nu = \frac{3\gamma-1}{\gamma-1}$. From (29)-(32), it is very clear that except the entropy expression, all remain unchanged with respect to the case of a non-rotating central object. Also from (30) and (32), we get the shock invariant quantity as

$$C = \frac{\left(\frac{2}{M_+} + (3\gamma-1)M_+ \right)^2}{M_+^2(\gamma-1) + 2} = \frac{\left(\frac{2}{M_-} + (3\gamma-1)M_- \right)^2}{M_-^2(\gamma-1) + 2}, \quad (33)$$

which remains unchanged with respect to a non-rotating case. If only all the conditions, (29)-(31) and (33) are simultaneously satisfied by the matter, shock will be generated in an accretion disk.

4 GLOBAL ANALYSIS OF THE PARAMETER SPACE

One of our aim is to check, how does the rotation of GOHS affect the disk parameter region known for non-rotating case. More precisely, we will check, how does the rotation of GOHS affect the sonic location, structure as well as the stability of disk. As mentioned in §1, we will follow the methodology adopted by Chakrabarti (1996b) for global solution and Mukhopadhyay & Chakrabarti (2001) for stability analysis. In Fig. 1, we show the

variation of disk entropy as a function of sonic location. The intersection to the horizontal line (which indicates a constant entropy curve) with all the curves indicate the sonic points of the accretion disk for that particular entropy and rotation to the GOHS. It is clearly seen that at a particular entropy, if the co-rotation of GOHS increases, the inner sonic points shift to more inner edge of the disk, which are comparatively unstable region (because, beyond of x_s , disk orbit is not stable and decrement of the value of x_s is slower than that of x_c with J). For $J = 0.5$, the inner sonic point disappears, as we see that dashed curve terminates on the radial axis at $x_c \sim 6$ and it does not turn up to give rise the inner sonic point. The reason behind it is that, for higher the co-rotation, the angular momentum of the system will become higher and radial matter speed will be unable to overcome the centrifugal barrier close to the GOHS and that will make the disk unstable at the inner edge. For the counter-rotating cases, if J increases in magnitude for a particular entropy, disk will become more stable, as the radial speed will be able to overcome the centrifugal barrier at a larger radius compared to a co-rotating case and matter may attain supersonic speed at a larger distance, which is more stable region of the disk. However, for a high counter rotation, angular momentum of the system will become too low and the accretion will tend to 'Bondi-like flow' (Bondi 1952) with the existence of single sonic point.

It is seen that for $\alpha = 0-0.1$, the variation of curves are almost same and only significant changes come into the picture for $\alpha > 0.1$. Also for the lower viscosity, if the co-rotation is high (J is high), the possibility to have the all three sonic points in the disk is high. As the viscosity increases, the possibility for the existence of all three sonic points diminishes. In order to preserve the existence of sonic point for the high viscous cases, J must reduce to zero and subsequently, more negative. As a whole, from Fig. 1a-c we can conclude that for lower α , multiple sonic points may exist, but for high α , there is only one sonic point which is inner one in the accretion disk. Similar features come out from Fig. 2 but in terms of energy of the sonic point in accretion disk. As we know that the observed angular frequency for the candidate 4U 1636-53 is 582Hz, which is equivalent to $J = 0.2877$, one of the value of J chosen for our discussion is 0.2877. For both Fig. 1 and 2, sonic points with negative slope of the curve indicate the locations of 'saddle-type' or 'X-type' sonic point and positive slopes indicate the 'centre-type' or 'O-type' sonic point. Thus, the rotation of GOHS and viscosity of the disk are the important factors to the formation and location of sonic points, which are related to the structure of accretion disk.

Figure 3 indicates the variation of energy with entropy at sonic locations, when J is

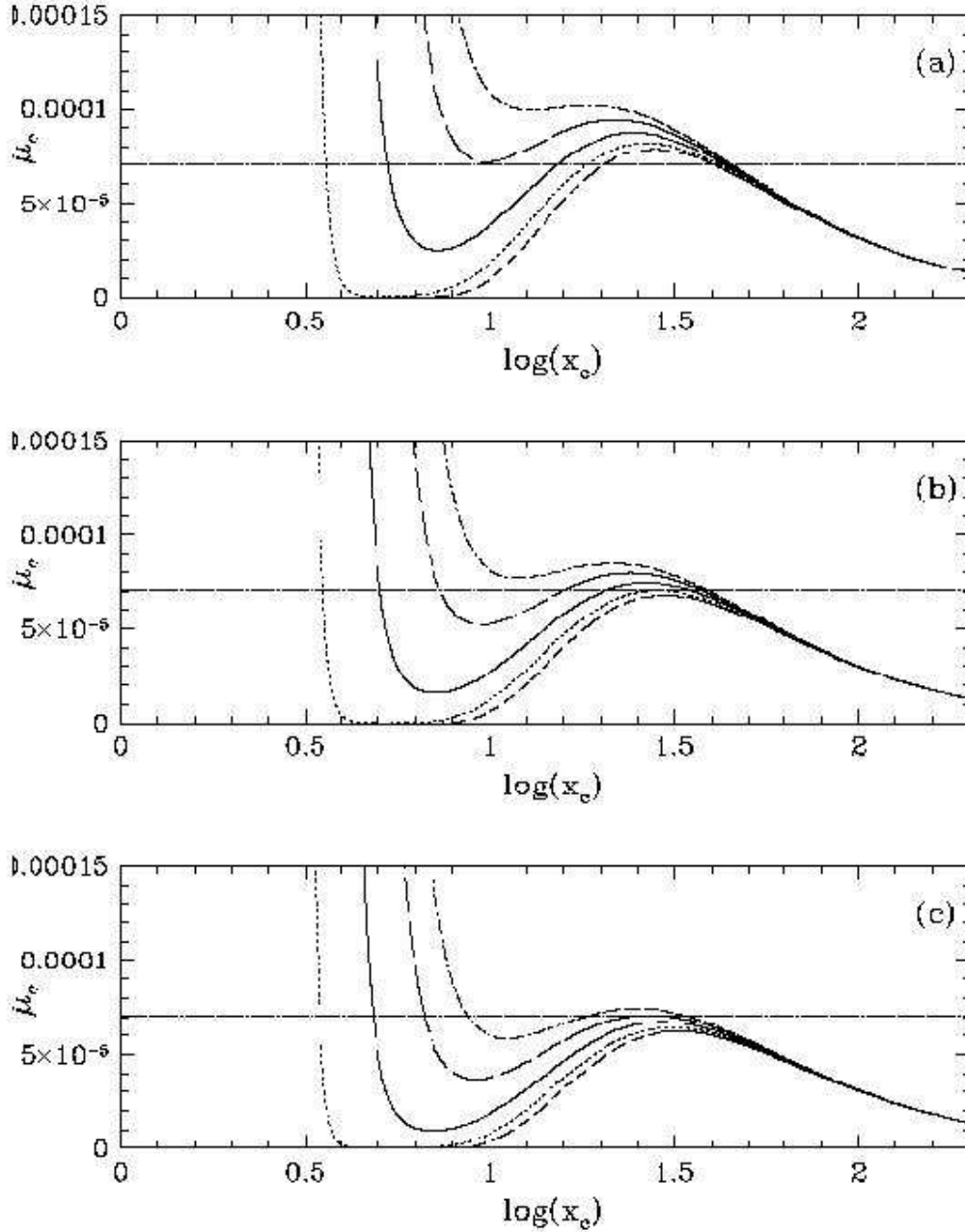


Figure 1. Variation of sonic entropy as a function of sonic location for various values of J when (a) $\alpha = 0, f = 0$, (b) $\alpha = 0.4, f = 0.5$, (c) $\alpha = 0.8, f = 0.5$. Central solid curve indicates non-rotating case ($J = 0$), while the dotted and dashed curves are for $J = 0.2877, 0.5$ respectively and long-dashed and dot-dashed curves are for $J = -0.2877, -0.5$ respectively. The horizontal line indicates the curve of constant entropy of 7×10^{-5} . The other parameters are $\lambda = 3.3, \gamma = 4/3$.

parameter for different viscosity of the fluid. It is seen that, with the increase of J (co-rotation), inner sonic points of the disk shift towards the lower entropy region keeping the outer sonic points unchanged and the disk becomes unstable. We know that the shock in accretion disk can be formed only if there is a possibility of matter in the outer sonic point

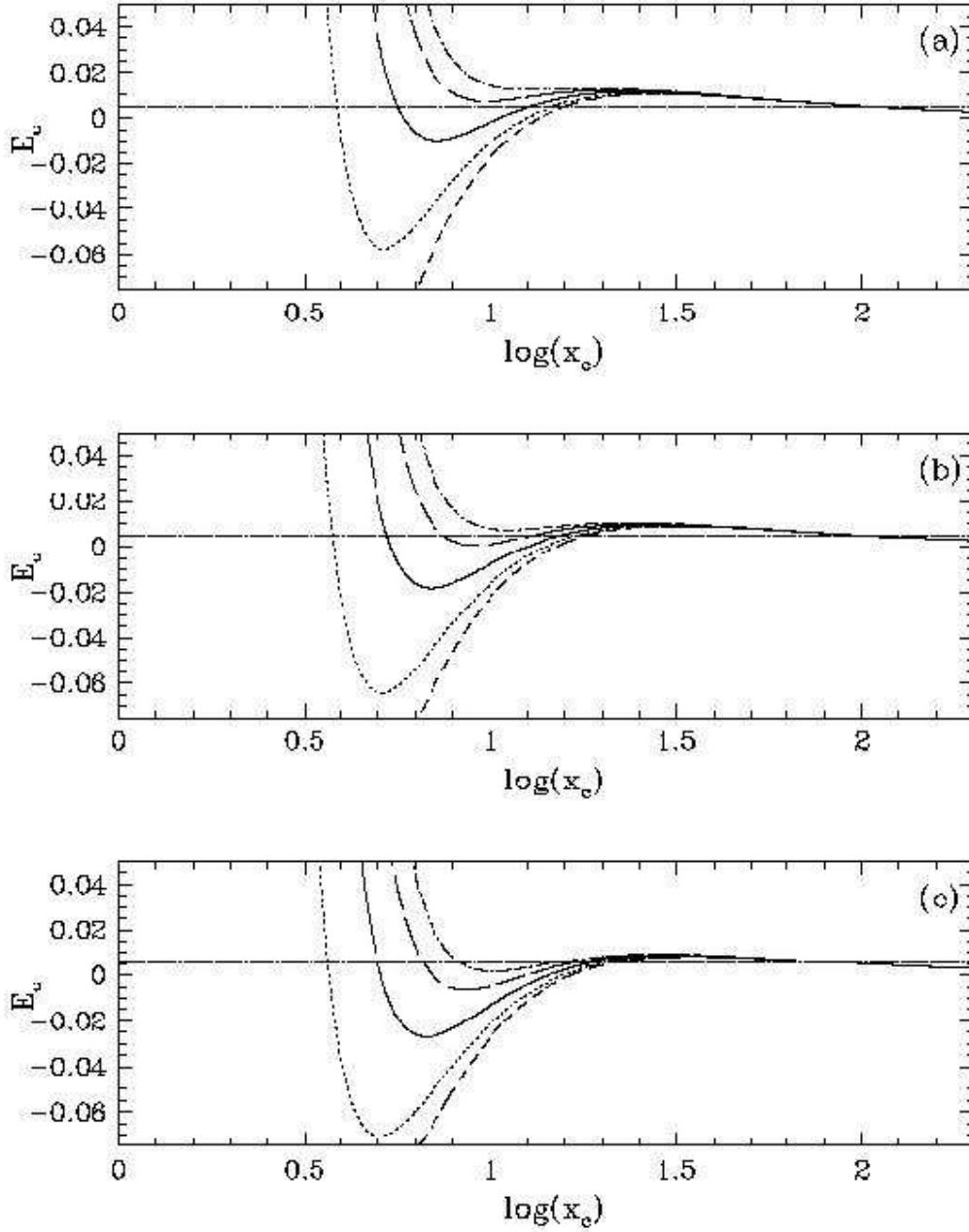


Figure 2. Same as 1, but sonic energy is plotted in place of entropy. The horizontal line indicates the curve of constant energy of 0.005.

branch of lower entropy to jump to the inner sonic point branch of higher entropy. As because, with the increase of J , inner sonic point branch itself shifts to the lower entropy region which is comparatively unstable, the shock as well as disk also become unstable. For $J = 0.5$, the inner sonic point branch disappears totally and only outer and O-type sonic point branches remain. Clearly, for a highly rotating GOHS, the possibility of formation of

shock reduces as well as the shock becomes unstable, as the inner sonic point branch itself disappears or tends to disappear. The physical reason behind it is that, with the increase of value of J , the angular momentum of the system increases, which helps the disk to maintain a high azimuthal speed of matter upto a very close radius to the GOHS, as a result the radial speed of the matter can overcome the corresponding sound speed at a very inner radius only. On the otherhand, the inner edge of the accretion disk is comparatively less stable, as the entropy decreases at lower radii. As the sonic points form at a more inner radii, with the increase of J , disk tends to an unstable situation.

In case of the counter-rotation of GOHS, as J increases in magnitude, the inner sonic point branch shifts towards a higher entropy region, and the disk as well as the shock become more stable. The physical reason to have a more stable inner sonic point branch for the counter-rotating case is the following. As the counter rotation of central object increases, that is the angular momentum of the system reduces, the matter falls freely towards GOHS at larger radii and it becomes supersonic at a comparatively outer edge of the disk. Thus, the disk as well as shock become more stable. However, for a very high counter-rotation of GOHS, this inner sonic point branch itself tends to merge to the outer sonic point branch, and the entire system shift towards the outer side which is more stable. As in case of higher counter-rotation, the angular momentum of the system becomes very small, the corresponding centrifugal pressure onto the matter becomes insignificant, as a result the possibility of shock diminishes again. Thus, if the angular momentum of GOHS increases or decreases significantly, the shock wave in accretion disk becomes unstable and the disk itself tends to an unstable situation. In Fig. 3, 'C' is the point, where the flow can pass through the inner and outer sonic point simultaneously. The parameters around C are important to study the shock in accretion disk.

As the viscosity of flow increases, the possibility of intersection between inner and outer sonic point branch decreases. With the increase of viscosity, more regions containing the X-type sonic points become O-type. The outer X-type sonic points recedes in further out and inner one proceeds in further inwards. Also for higher viscosity, the outer sonic points may no longer remain as X-type and only the inner sonic points may exist. Thus, the possibility of shock will reduce.

5 FLUID PROPERTIES OF ACCRETION DISK

Now we will discuss the behaviour of viscous accreting fluid around rotating GOHS. In the previous section, we have already confirmed that the rotation significantly affects the global parameter space of accretion disk. Here, our intention is to see, how the various fluid dynamical results of an accretion disk are affected for various values of J and α . For a certain choice of physical parameter set, if the existence of sonic radii are possible in the accretion disk around GOHS, the flow structures can be studied for the corresponding choice of sonic radii (or energy) of the accretion flow.

In Fig. 4a, we show the variation of Mach number for three different values of J at a particular viscosity. As the viscosity is low, the rate of energy momentum transfer in matter is less. It is known that for an accretion around neutron star, in a certain cases, matter may be always subsonic (Chakrabarti & Sahu 1997; Mukhopadhyay 2002a) and at the stellar surface matter speed reduces to zero. Owing to this fact, here such a situation is considered where the speed of the accreting fluid is low, which accounts for the high residence time of matter in the disk. The angular momentum of the disk is high at $x \sim 10$ (see Fig. 4d) and thus radial matter speed is low. Subsequently, though the disk angular momentum goes down, as the matter comes closer to the stellar surface, it starts to decelerate and the radial matter speed still remains low. This results to a higher the possibility of cooling, and thus cooling factor f is chosen as 0.1. As the energy momentum transfer rate of matter is low, the accretion rate is chosen intermediate. We have chosen a standard mass of GOHS as $2M_{\odot}$. If the GOHS is chosen to be non-rotating, angular momentum of the system is less and the centrifugal barrier is minimum. With the increase of J , this centrifugal barrier increases, and it becomes very high particularly for $J = 0.5$. Mach number profiles clearly indicate that at the surface of GOHS, accreting fluid stops. Also from Fig. 4b and 4c, it comes out that sudden deceleration of the accreting fluid gives rise to a sudden enhancement of density and temperature close to GOHS. Here, the temperature is thought to be cooled down by a factor of 1/30 through the inverse-Compton effect in the radiation pressure dominated relativistic flow. Thus, we choose $\beta \sim 0.03$. Nevertheless, the temperature is still very high, which was also reported earlier (Mukhopadhyay 2002a) in the context of non-rotating neutron star. The density profiles are plotted in unit of $\frac{c^6}{G^3 M^2}$. Figure 4d shows the ratio of sub-Keplerian to Keplerian angular momentum variation of the accreting fluid as a function of radial coordinate. It is seen that, at the boundary between Keplerian and sub-Keplerian

disk, $\lambda_k/\lambda \rightarrow 1$, and from that radius (x_K) we start our calculation as our discussion is for sub-Keplerian accretion disk. From the λ_k/λ profile, it is again clear that for higher J , centrifugal barrier becomes stronger. Far away from GOHS, the effect of centrifugal barrier is weak, but as the matter approaches towards GOHS, it starts to dominate and at $x \sim 10$ it becomes stronger. Then again it goes off. However, at very close to the GOHS, again this centrifugal effect comes into the picture as the matter falls into the strong rotational field of GOHS. This effect appears very prominently for high value of J , which is here chosen to be 0.5. Actually, this effect comes into the picture, once the matter enters into the corresponding ergosphere of HT geometry. But the important point to be noted that if the outer radius of GOHS is greater than the radius of ergosphere, this feature is not possible to occur.

In Fig. 5, we show the results of accretion phenomena for 4U 1636-53, whose angular momentum $J = 0.2877$. The examples are shown, where the sonic point(s) exist in the flow and shock forms in the accretion disk around 4U 1636-53 for different viscosity parameters. Figure 5a shows the variation of Mach numbers as a function of radial coordinate. It reflects that, for a small α (~ 0) only shock is possible at $x = 19.02$ in the accretion disk. As α increases, the energy momentum transfer rate increases, rate of infalling the matter enhances and velocity of the accreting fluid becomes high at the inner edge of the disk. But, because of the inner hard surface, matter has to stop at close to GOHS and naturally another shock forms at the inner edge of the accretion disk. The shock locations for $\alpha = 0.02$ and 0.05 , are at $x = 14.27, 4.38$ and $x = 15.37, 4.31$ respectively. If the viscosity is high, the cooling factor is intermediate (see Fig. 5 caption). Also, the angular momentum of matter at the sonic point is chosen as, $\lambda_c = 3$, and for the radiation dominated, inverse-Comptonised flow, β is chosen to be 0.03. Figures 5b and 5c show the variations of density and temperature. The regions, where velocity decelerates abruptly, temperature and density also jumps up in a significant manner. Here also, the inverse-Comptonised temperature is very high as the cases of Fig. 4.

6 SUMMARY AND DISCUSSION

Here, we have studied the viscous accretion phenomena around rotating gravitational object with hard surface (GOHS), i.e., mostly around compact object like neutron star and strange star. We started with a proposal of a new pseudo-Newtonian potential by means of Hartle-Thorne geometry, as this metric can describe the space-time of interior as well as exterior

to a slowly rotating star. We have shown that this potential can describe all the essential relativistic properties like, radius of marginally bound and stable orbit, specific mechanical energy etc., of accretion disk within 10% error. Then, along with this potential, we have described the accretion disk by using non-relativistic equations. Therefore, we can say, our method is a 'pseudo-general-relativistic'. Once the pseudo-Newtonian potential is proposed, we have applied it to the study of relativistic fluid properties of accretion disk around rotating GOHS. We have prescribed the set of basic equations for vertically averaged, thin, viscous accretion disk. Then, we have analysed the viscous parameter space globally. Subsequently, we have discussed about the properties of viscous fluid and the effect of rotation on the fluid behaviour. Examples are shown for the accretion disk around an observed candidate 4U 1636-53, which is one of the fast rotating compact object with angular frequency 582Hz (equivalent $J = 0.2877$). As starting from a new pseudo-potential, we have discussed upto the solution of viscous accretion flow, this is one of the most self consistent paper on accretion disk.

We have studied the stability of accretion disk. Most of the earlier analysis of structure and stability of the accretion disk have been done around non-rotating central object. As no cosmic object is static, it is very important to consider the effect of rotation, particularly for the discussion of an inner edge of the disk. We have found that, when the rotation to a GOHS is incorporated, the locations of sonic point (if any) get shifted to the unstable region and the shock (if any) gets affected in the disk, and thus the disk structure gets influenced. Therefore, we can conclude that the rotation should be incorporated in the study of an accretion disk. Any related conclusion is dependent on the rotation parameter of GOHS. The mentioned disk properties and phenomena not only get modified and/or shifted in location, sometimes disappeared completely. Prasanna & Mukhopadhyay (2003), worked on the stability analysis of accretion disk around rotating compact objects in a perturbative manner. They incorporated the rotational effect of central object in a disk indirectly by the inclusion of Coriolis acceleration term. Here, this rotational effect is brought directly from the metric itself.

From the global analysis of sonic points, we have seen that for a higher co-rotation of GOHS, the disk becomes unstable for a particular angular momentum of the accreting matter. As the formation of shock needs a stable inner sonic point in the accretion disk, for the higher value of J , shock is unstable as the inner region of disk is unstable. On the other hand, for counter-rotating cases, the angular momentum of system reduces and the matter

falls more strongly to a GOHS. As there is no significant centrifugal barrier to slow down the matter in disk, the possibility of shock reduces again. Also the branch of inner sonic point merges or tends to merge to that of outer sonic point. Thus, we can conclude that the parameter region, where the shock is expected to form for non-rotating GOHS (Chakrabarti & Sahu 1997), is affected for rotating ones and the possibility of shock is reduced for both the co-rotating and counter-rotating GOHS. Also for the higher viscosity, both the inner and outer sonic point branch merge each other and the possibility of shock reduces again. Actually, with the increase of viscosity, the region containing the X-type sonic points tends to become O-type. The outer X-type sonic points recede in more outwards and inner ones proceed in inwards more.

As the incoming matter slows down abruptly at the surface of GOHS as well as at two shock locations (if two shocks form), the overall density becomes higher for an accretion disk around GOHS compared to that for a black hole. Similarly, the temperature in the disk is higher for a GOHS. Thus, one can conclude that the accretion disk around a GOHS is very favourable for nucleosynthesis. We know that the accretion disk around a black hole is enough hot for nucleosynthesis (Mukhopadhyay 1999; Mukhopadhyay & Chakrabarti 2000), which are different from that in star. As the density and temperature may be much higher around a GOHS, more efficient nucleosynthesis is expected particularly at an inner region of the disk. In early, we saw that the high temperature of accretion disk around a black hole is very favourable for the photo-dissociations and the proton capture reactions (Chakrabarti & Mukhopadhyay 1999). As the accretion disk around a GOHS is hotter than that around a black hole, even ${}^4\text{He}$ which has a high binding energy, may dissociate into deuterium and then into proton and neutron. If we consider the accreting matter to come from the nearby 'Sun like' companion star, the initial abundance of ${}^4\text{He}$ in the accreting matter is supposed to be about 25%. Therefore, by the dissociation of this ${}^4\text{He}$, neutron may produce in a large scale, which could give rise to the neutron rich elements. Guessoum & Kazanas (1999) showed that the profuse neutron may be produced in the accretion disk and through the spallation reactions *lithium* may be produced in the atmosphere of the star. When the neutron comes out from the accretion disk by the formation of an outflow, in that comparatively cold environment, ${}^7\text{Li}$ may be produced which can be detected on the stellar surface. In early, it was shown that the metalicity of the galaxy may be influenced when outflows form in the hot accretion disk around black holes (Mukhopadhyay & Chakrabarti 2000). In case of the lighter galaxy, the average abundance of the isotopes of *Ca*, *Cr* may

significantly change. Also the abundance of lighter elements, like the isotopes of *C*, *O*, *Ne*, *Si* etc. may increase significantly. As the temperature of the accretion disk around GOHS is higher, the expected change of abundance of these elements and the corresponding influence on the metallicity of the galaxy is expected to be high.

We know that, out of an observed pair of kilohertz QPO frequencies for a particular candidate, one is the oscillation due to its Keplerian motion (Osherovich & Titarchuk 1999). For 4U 1636-53, lower frequency is 950Hz (Wijnands et al. 1997) which may be the Keplerian one. According to our pseudo-potential, if we calculate this Keplerian frequency for 4U 1636-53, it comes out to be 1027Hz for $M = 1.4M_{\odot}$ and $x_K = 18$, which is not much over estimated with respect to the observed one. Thus, we can give a theoretical prediction of QPO, at least for one, out of a pair. Similarly, for other candidates, one can calculate Keplerian frequency according to our potential and compare with observation. The detailed theoretical study of QPO based on this present scheme will be pursued elsewhere.

ACKNOWLEDGMENTS

SG is thankful to Inter-University Centre for Astronomy and Astrophysics for Summer Training Programme, 2002, where this work was initiated.

REFERENCES

- Abramowicz, M., Chen, X.-M., Granath, M., & Lasota, J.-P. 1996, ApJ, 471, 762
Abramowicz, M., Czerny, B., Lasota, J., & Szuszkiewicz, E. 1988, ApJ, 332, 646
Abramowicz, M., & Kato, S. 1989, ApJ, 336, 304
Artemova, I., Björnsson, G., & Novikov, I. 1996, ApJ, 461, 565
Bondi, H. 1952, MNRAS, 112, 195
Chakrabarti, S. K. 1989, ApJ, 347, 365
Chakrabarti, S. K. 1990, Theory of Transonic Astrophysical Flows. World Scientific
Chakrabarti, S. K. 1996a, ApJ, 464, 664
Chakrabarti, S. K. 1996b, MNRAS, 283, 325
Chakrabarti, S. K. 1996c, ApJ, 471, 237
Chakrabarti, S. K., & Mukhopadhyay, B. 1999, A&A, 344, 105
Chakrabarti, S. K., & Sahu, S. 1997, A&A, 323, 382
Cox, J., & Giuli, R. 1968, Principles of Stellar Structure. Gordon & Breach, New York
Gammie, C., & Popham, R. 1998, ApJ, 498, 313
Guessoum, N., & Kazanas, D. 1999, ApJ, 512, 332
Hartle, J. B., & Thorne, K. S. 1968, ApJ, 153, 807
Kato, S., Fukue, J., & Mineshige, S. 1998, Black Hole Accretion Discs. Kyoto University Press
Landau, L., & Lifshitz, E. 1987, Fluid Mechanics. Butterworth-Heinemann

- Lovas, T. 1998, *IJMPD*, 7, 471
- Lu, J.-F., Yuan, F. 1998, *MNRAS*, 295, L66
- Lynden-Bell, D. 1969, *Nature*, 223, 690
- Manmoto, T. 2000, *ApJ*, 534, 734
- Matsumoto, R., Kato, S., Fukue, J., & Okazaki, A. 1984, *PASJ*, 36, 71
- Miwa, T., Fukue, J., Watanabe, Y., & Katayama, M. 1998, *PASJ*, 50, 325
- Mukhopadhyay, B. 1999, *Ind. J. Phys.*, 73B, 917; astro-ph/9910080
- Mukhopadhyay, B. 2000, *Proceedings of 9th Marcel Grossman Meeting, Rome, 2000* (World Scientific); astro-ph/0103162
- Mukhopadhyay, B. 2002a, *IJMPD*, 11, 1305; astro-ph/0203438
- Mukhopadhyay, B. 2002b, *ApJ*, 581, 427; astro-ph/0205475
- Mukhopadhyay, B., & Chakrabarti, S. K. 2000, *A&A*, 353, 1029
- Mukhopadhyay, B., & Chakrabarti, S. K. 2001, *ApJ*, 555, 816
- Mukhopadhyay, B., & Misra, R. 2003, *ApJ*, 582, 347; astro-ph/0209042
- Narayan, R., Barret, D., & McClintock, J. 1997, *ApJ*, 482, 448
- Narayan, R., Mahadevan, R., Grindlay, J., Popham, R., & Gammie, C. 1998, *ApJ*, 492, 554
- Narayan, R., & Yi, I. 1994, *ApJ*, 428, L13
- Novikov, I., & Thorne, K. 1973, *Black Holes, Les Houches 1972* (France), ed. B. & C. DeWitt. Gordon & Breach, New York, 343
- Nowak, M. A., & Wagoner, R. V. 1991, *ApJ*, 378, 656
- Osheroich, V., & Titarchuk, L. 1999, *ApJ*, 522, L113
- Paczynski, B., & Wiita, P. 1980, *A&A*, 88, 23
- Peitz, J., & Appl, S. 1997, *MNRAS*, 286, 681
- Popham, R. & Gammie, C. 1998, *ApJ*, 504, 419
- Popham, R., & Sunyaev, R. 2001, *ApJ*, 547, 355
- Prasanna, A. R., & Mukhopadhyay, B. 2003, *IJMPD*, 12, 157; astro-ph/0107119
- Pringle, J., & Rees, M. 1973, *A&A*, 21, 1
- Semerák, O., & Karas, V. 1999, *A&A*, 343, 325
- Shakura, N., & Sunyaev, R. 1973, *A&A*, 24, 337
- Sponholz, H., & Molteni, D. 1994, *MNRAS*, 271, 233
- Strohmayer, T., & Markwardt, C. 2002, *ApJ*, 577, 337
- Wijnands, R., van der Klis, M., van Paradijs, J., Lewin, W., Lamb, F., Vaughan, B., & Kuulkers, E. 1997, *ApJ*, 479, L141

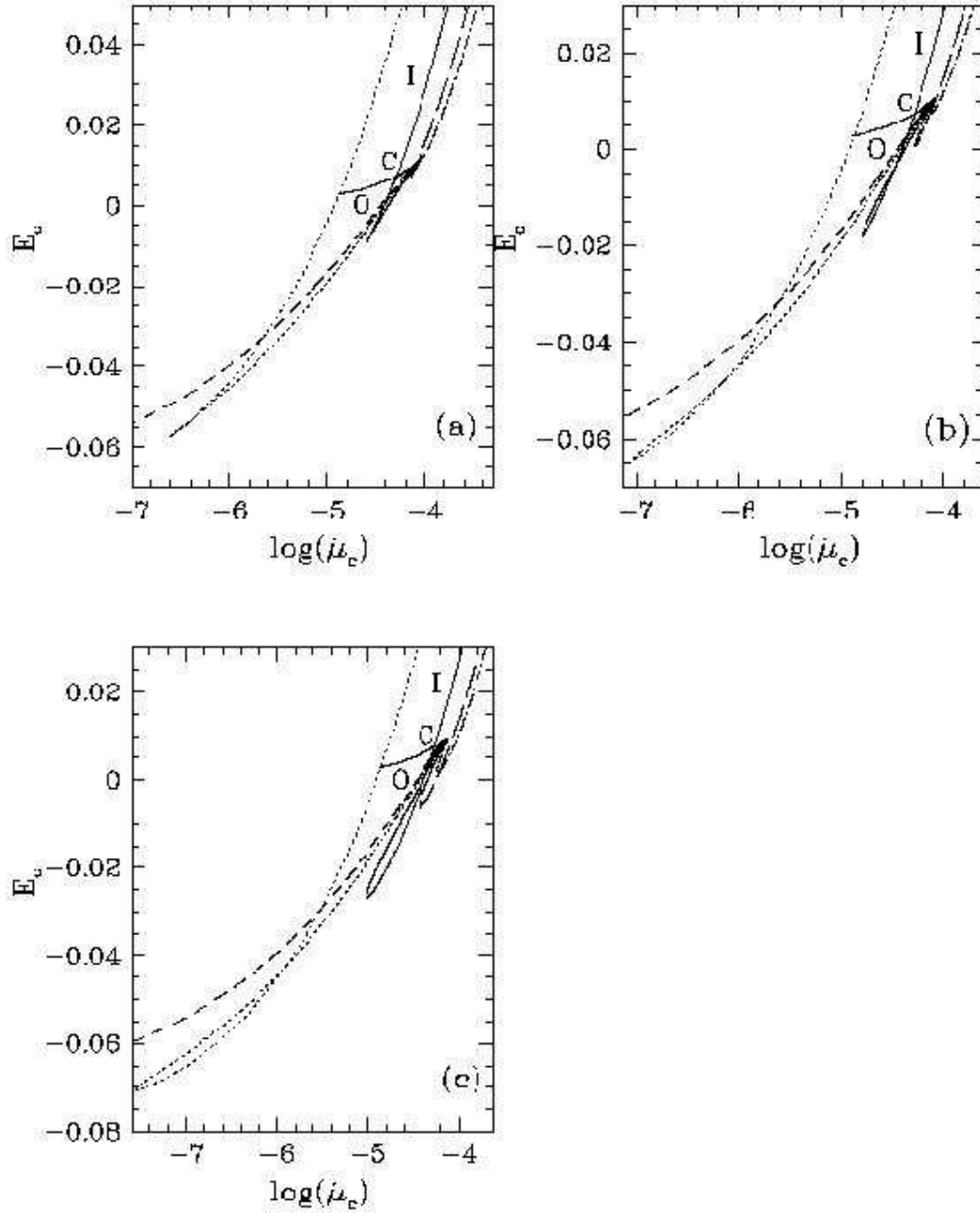


Figure 3. Variation of sonic energy as a function of sonic entropy for various values of J when (a) $\alpha = 0, f = 0$, (b) $\alpha = 0.4, f = 0.5$, (c) $\alpha = 0.8, f = 0.5$. Solid curve indicates non-rotating case ($J = 0$), while the dotted and dashed curves are for $J = 0.2877, 0.5$ respectively and long-dashed and dot-dashed curves are for $J = -0.2877, -0.5$ respectively. O and I indicate the locus of outer and inner sonic point respectively, while C is the intersection of outer and inner sonic point locus. The other parameters are $\lambda = 3.3, \gamma = 4/3$.

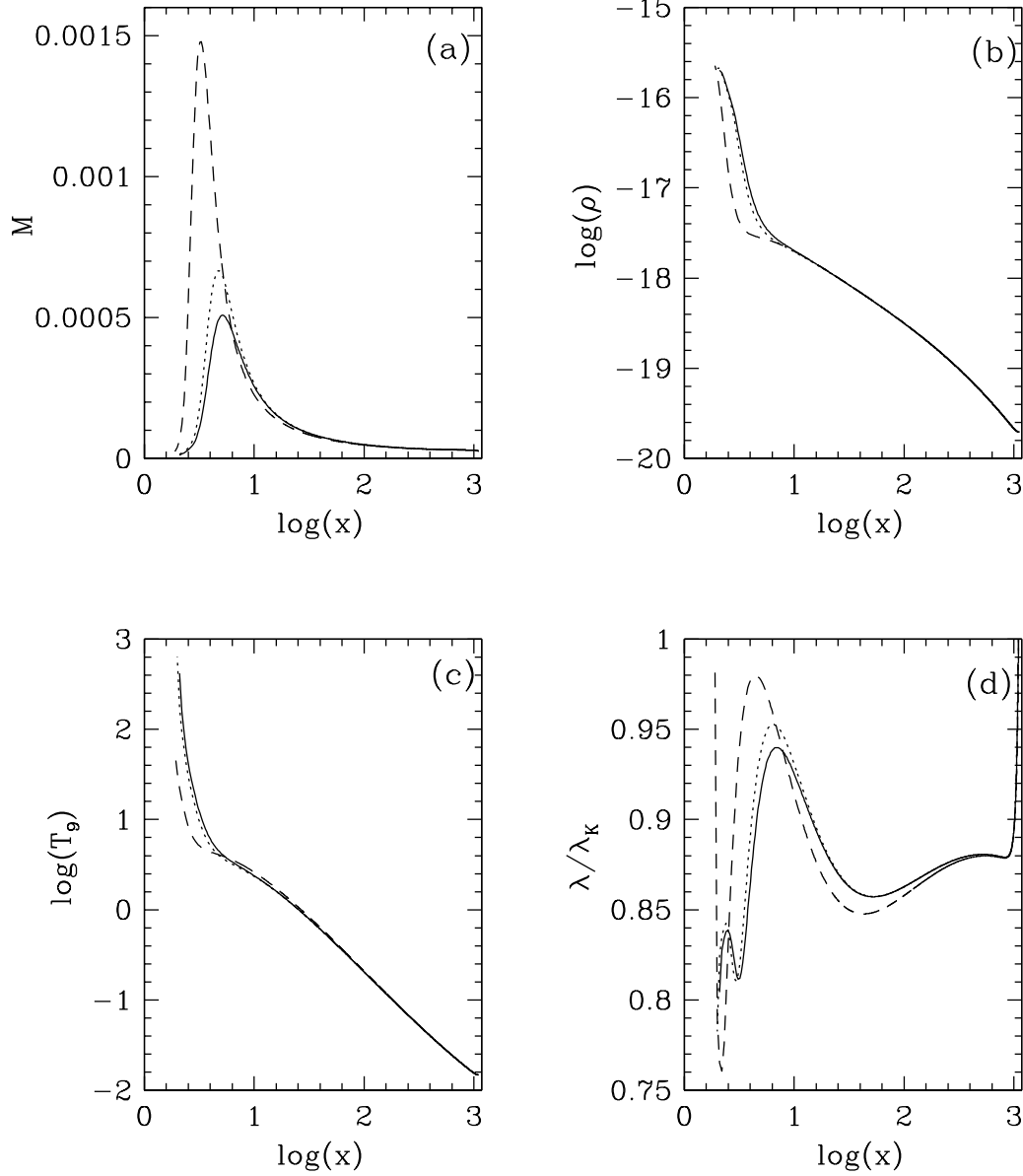


Figure 4. Variation of (a) Mach number, (b) density, (c) temperature in unit of 10^9 , (d) ratio of sub-Keplerian to Keplerian angular momentum of the accreting fluid as a function of radial coordinate. Solid, dotted and dashed curves are for $J = 0, 0.1, 0.5$ respectively. Other parameters are $\alpha = 0.0001, f = 0.1, M = 2, \dot{M} = 2, \beta = 0.03$.

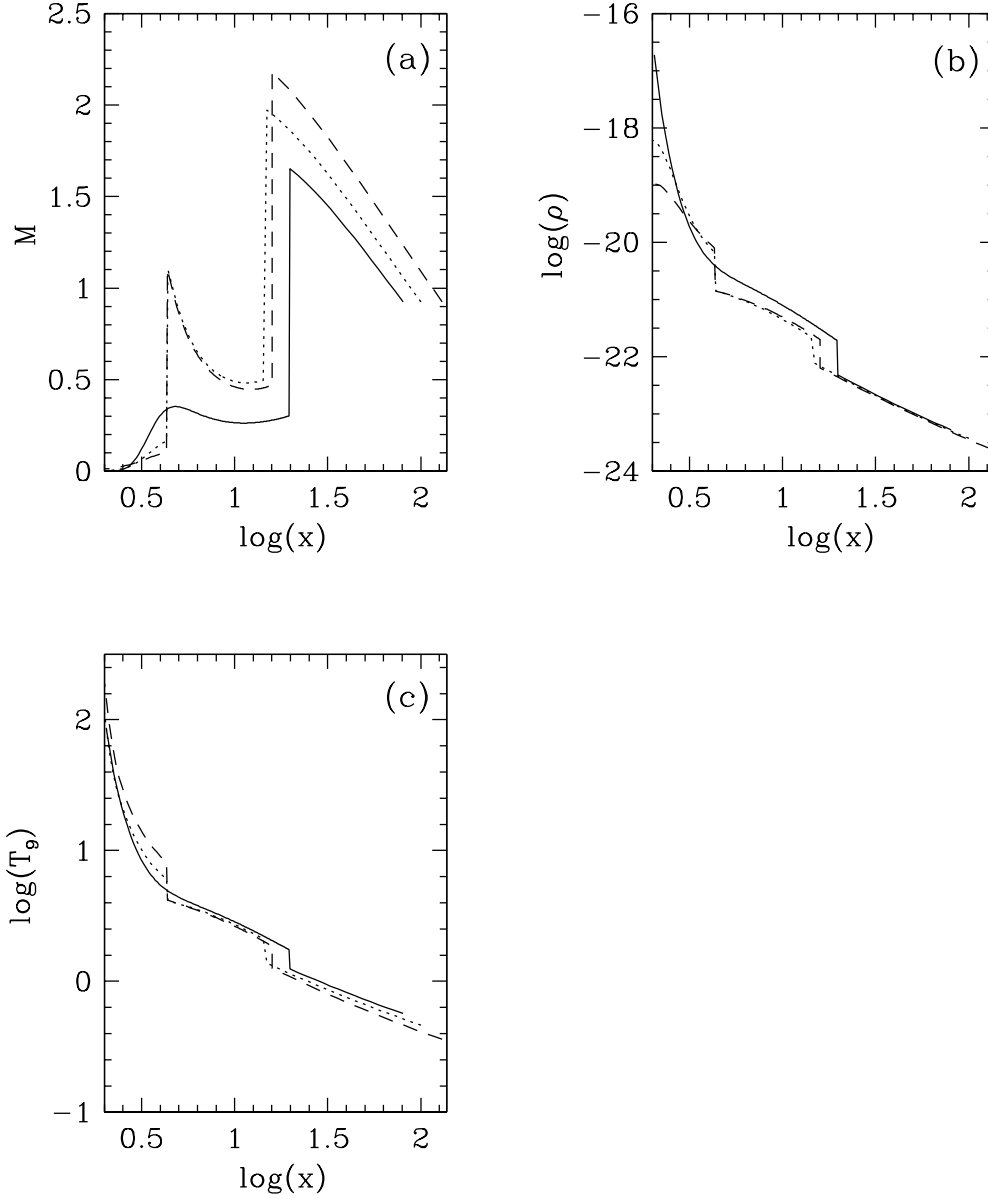


Figure 5. Variation of (a) Mach number, (b) density, (c) temperature in unit of 10^9 as a function of radial coordinate for the accretion disk around 4U 1636-53. Solid, dotted and dashed curves are respectively for (i) $\alpha = 0, f = 0$, (ii) $\alpha = 0.02, f = 0.2$, (iii) $\alpha = 0.05, f = 0.5$. Other parameters for 4U 1636-53 are $J = 0.2877, \lambda_c = 3, M = 1.4, \dot{M} = 1, \beta = 0.03$.